Robotica (2000) volume 18, pp. 201–208. Printed in the United Kingdom © 2000 Cambridge University Press

Nonlinear dynamics of a single-degree robot model Part 2: Onset of chaotic transients

V. Paar*, N. Pavin*, N. Paar* and B. Novaković†

(Received in Final Form: June 28, 1999)

SUMMARY

In Part 1 of this paper[1] we have investigated numerically the quasiperiodic and frequency locked solutions of mathematical model of a robot with one degree of freedom. In this paper we extend our investigations to the region of transient chaos. The zones of chaotic transients are very broad and lie beyond the parameter range of engineering significance. Transiently chaotic zones exhibit a complex structure, fractally intertwined with tongues of regular pattern and cover a broad range of control parameter L. The crisis point for the onset of sustained chaos lies extremely far from the point of onset of transient chaos.

KEYWORDS: Robot models; Damping; Nonlinear dynamics; Transient chaos; Crisis point; Sustained chaos.

1. INTRODUCTION

In order to avoid potentially adverse errors, industrial designers must be prepared to devote a greater effort into exploring the full range of possible dynamic responses of their systems.[2] In particular, it is important to know quantitatively where in the parameter space the simple period 1 solution (with the period of the external driver) becomes unstable; this is of importance for the construction of devices on the basis of nonlinear oscillator which should operate reliably, with the generation of complicated periodic motion or chaotic noise. It is well known that even simple mathematical models of nonlinear dynamics can exhibit surprisingly complex behavior.[3–7]

The periodic forcing of nonlinear oscillators has been, in particular, a topic of broad interest to basic scientists and engineers.[3,7–12]

In a previous paper (Part 1) we have introduced a mathematical model for a robot with one degree of freedom,[1] based on considerations of dynamics of a full robot (manipulator plus actuators), incorporating relevant mechanical parameters.[13–18] It was shown that the resulting mathematical model corresponds to the following simple form:

$$\ddot{x} - \beta_2 \dot{x}^2 sgn(\dot{x}) - \gamma_2 sgn(\dot{x}) - \delta_{21} x - \delta_{23} x^3 = L\frac{\omega_0^2}{2\pi}\cos(\omega_0 t) - \xi_{21} e^{\lambda_{21} t} - \xi_{22} e^{\lambda_{22} t}. \quad (1)$$

* Department of Physics, Faculty of Science, University of Zagreb, Zagreb (Croatia)
† Faculty of Mechanical Engineering and Naval Architecture, University of Zagreb, Zagreb (Croatia)

The second and third term on the l.h.s. of Eq. (1) are dissipative terms, corresponding to the viscous and dry friction,[18] respectively. The parameters δ_{21} and δ_{23} are the coefficients of rigidity; the signs $\delta_{21} < 0$ and $\delta_{23} < 0$ correspond to the rigidity with the effect of a hard spring. The first term on the r.h.s. of the Eq (1) is the periodic driving force with driving frequency ω_0 and driving amplitude $L\omega_0^2/2\pi$, where L denotes the translation length. This term corresponds to the nominal control minimizing the Hamiltonian.[19] The last two terms present the feedback drive with the strengths given by:

$$\xi_{21} = \frac{a_2}{c_2} \cdot \lambda_{21}^2 ,$$

$$\xi_{22} = \frac{b_2}{c_2} \cdot \lambda_{22}^2 ,$$

$$a_2 = \lambda_{22} z_2(t_0) - z_4(t_0) ,$$

$$b_2 = z_4(t_0) - \lambda_{21} z_2(t_0) ,$$

$$c_2 = \lambda_{22} - \lambda_{21}, \quad \lambda_{22} \neq \lambda_{21}.$$

The parameters λ_{21} and λ_{22} denote the desired roots of the system in the regime of closed regulation loops.

The values of parameters in Eq. (1) were fixed at the values: $\omega_0 = 2\pi$, $\lambda_{21} = -10.5$, $\lambda_{22} = -11.5$, $\beta_2 = -5.18 \cdot 10^{-6}$, $\gamma_2 = -0.00298$, $\delta_{21} = -0.7611$, $\delta_{23} = -0.0127$, $z_2(0) = 0.01$, $z_4(0) = 0.01$. This parameterization was referred to as the parametrization (I). The length parameter L (in the units of length) was treated as a control parameter in computer simulations. Throughout the computations, the fixed initial conditions are taken $x_0 = 0$, $\dot{x}_0 = 0$. A particular parameter scan was adopted, close to the upper boundary of the estimated range of linear and cubic coefficients or rigidity. In Part 1[1] nonlinear aspects of dynamics of this mathematical model were numerically investigated in regular region in the length parameter – forcing frequency parameter plane and for sweeps through that plane.

Computations were performed using a network of DEC-3100 and ALPHA work stations. Differential equation (1) was solved using the D02BAF routine from the NAG library. This routine employs the Runge-Kutta method with automatic adjustments of numerical precision. The tolerance was fixed at 10^{-11}.

It was shown[1] that for an approximately small length parameter L, the system shows a limit cycle with period

https://doi.org/10.1017/S0263574799001952 Published online by Cambridge University Press

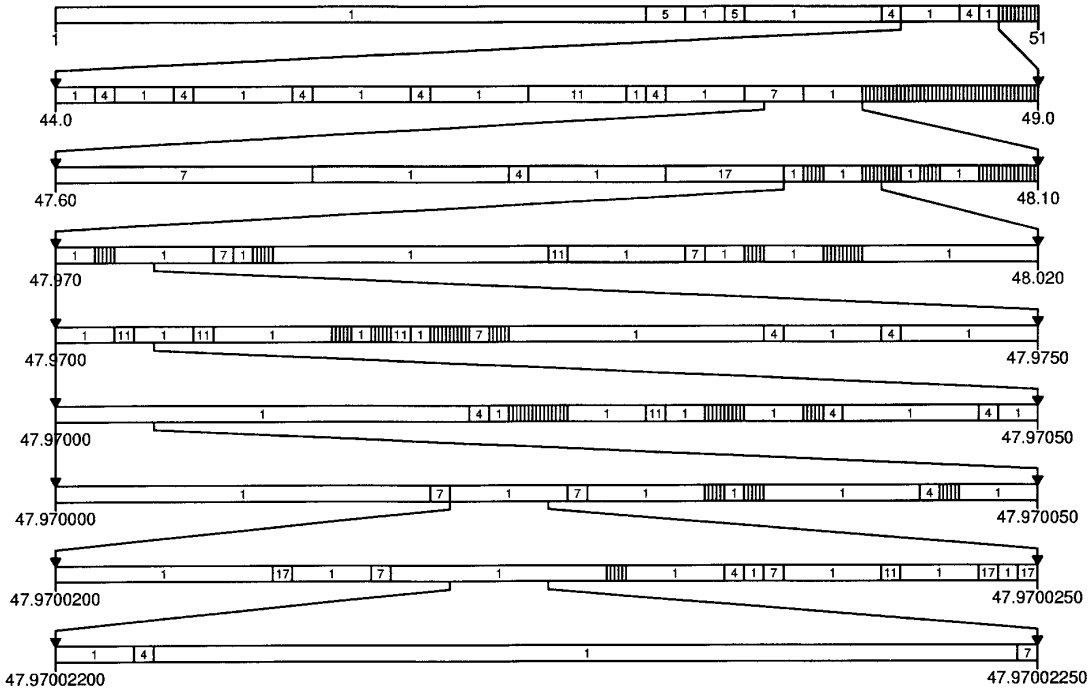

Fig. 1. Phase diagram showing the sweep through L for the system (1) at $\omega_0 = 2\pi$ and successive magnifications of some subintervals. In the first row the increment of L is $\Delta L = 1$. At each step of magnification, going from a row to row, the increment ΔL is decreased 10 times, i.e. the resolution is increased ten times. The label n denotes a solution with frequency locking of period n, and the chaotic transient is shown as dashed.

$T = \frac{2\pi}{\omega_0}$, i.e. the period-1 behavior. As L is gradually increased, the system exhibits the two-frequency quasiperiodic behavior, with a period-1 asymptote. The range of L which is of direct significance for engineering purposes, lies within this interval of L. Nonlinear effects in the neighboring regions of higher values of L in a particular parameter scan showed[1] a complex frequency locked and quasiperiodic structure with increasing L up to the point of appearance of chaotic transients (at $L \approx 48$ for $\omega_0 = 2\pi$).

2. DYNAMIC STRUCTURE IN THE REGION OF TRANSIENT CHAOS

In the present paper we investigate solutions of Eq. (1) in the region of transient chaos. Chaotic transients have been previously observed and investigated in various dynamical systems.[19–25] In dynamical system (1) the transient chaos appears for $\omega_0 = 2\pi$ at $L \approx 48$. In order to get an insight into the onset of this transient chaos, successive magnifications of the sweep through the control parameter L at $\omega_0 = 2\pi$ are presented in Figure 1.

At the level of resolution in the top row (the $L = 1$-50 interval with the increment $\Delta L = 1$), one observes two period-5 and two period-4 Arnold tongues prior to the onset of transient chaos at $L \approx 48$. The rest of the first row corresponds to a two-frequency quasiperiodic motion asymptoting into the period-1 solution, which is, therefore, labelled by 1. In the first step of magnification (second row), which magnifies the $L = 44$–49 subinterval, several additional Arnold tongues appear: four of period 4, one of period 7 and one of period 11. In the second step of magnification (third row), which magnifies the $L = 47.60$–48.10 subinterval, several additional tongues are observed: one of period 4, one of period 17 and three narrow chaotic tongues, etc. In each step, from one row to the next below, the resolution is increased ten times, revealing the tongue structure at smaller and smaller length scales. The repeated birth of narrow tongues can be seen under transformation of scale: at the level of finer resolution there appear narrower Arnold tongues and tongues of transient chaos. Each Arnold tongue of a particular period is getting splitted into a larger and larger number of narrower and narrower tongues of the same period. Similar fractal-type structure appears also for the quasiperiodic and transiently chaotic tongues in the same region, as indicated in Figure 1. Thus, in the region of onset of transient chaos there appears a fractal-type multiple structure of splitted Arnold tongues of some particular frequencies, tongues of quasiperiodicity (with period-1 asymptote) and tongues of chaotic transients.

This structure bears geometrical resemblance to the one found for the zones of sustained chaos in some dynamical systems with sizeable damping, as discussed, for example in Ref. 26.

The fractal-type pattern in Figure 1 is clearly seen from the map of the boundary between regular (frequency locked or periodic) and transiently chaotic zones in the phase diagram.

Figure 2(a) shows a 400×248 grid of (L, ω_0) parameters, ranging from $L = 45$ to $L = 49$ and from $\omega_0 = 6.222$ to $\omega_0 = 6.48$ in increments of $\Delta L = 0.001$ and $\Delta\omega_0 = 0.0010375$, respectively. At each of these lattice points on the parameter grid, the Eq. (1) was solved numerically and it was determined whether the solution is regular or transiently chaotic. The regular type of solution was indicated by a blank space and transiently chaotic by a dot in the parameter space. Such a map (and its successive magnifications) will be referred to as the phase space map of transient chaos.

https://doi.org/10.1017/S0263574799001952 Published online by Cambridge University Press

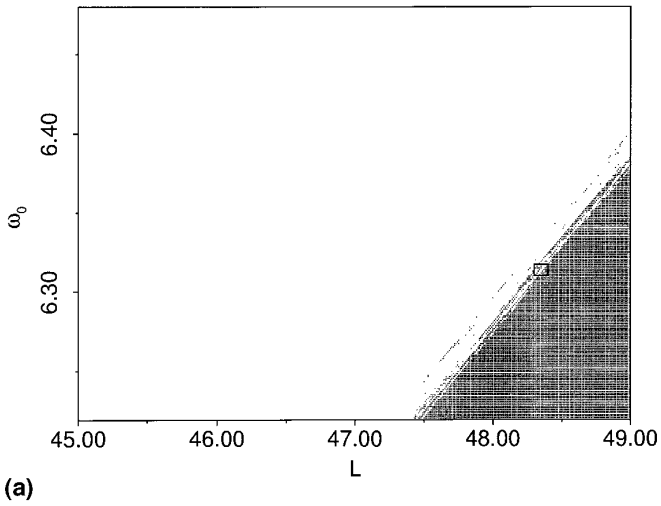

(a)

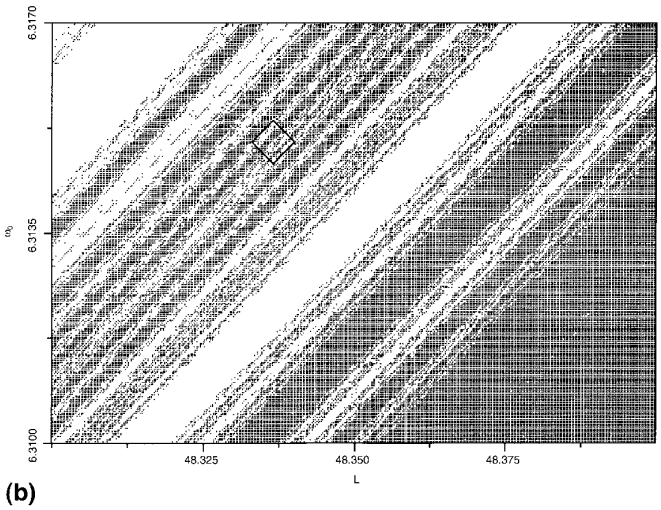

(b)

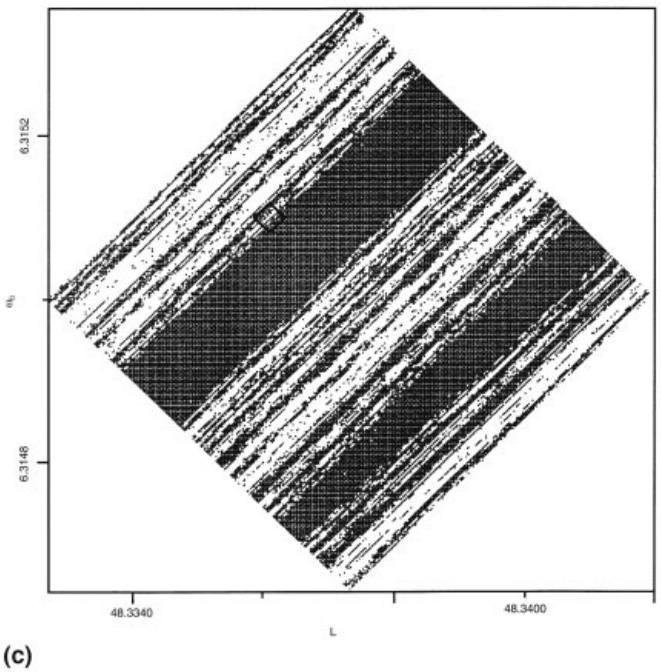

(c)

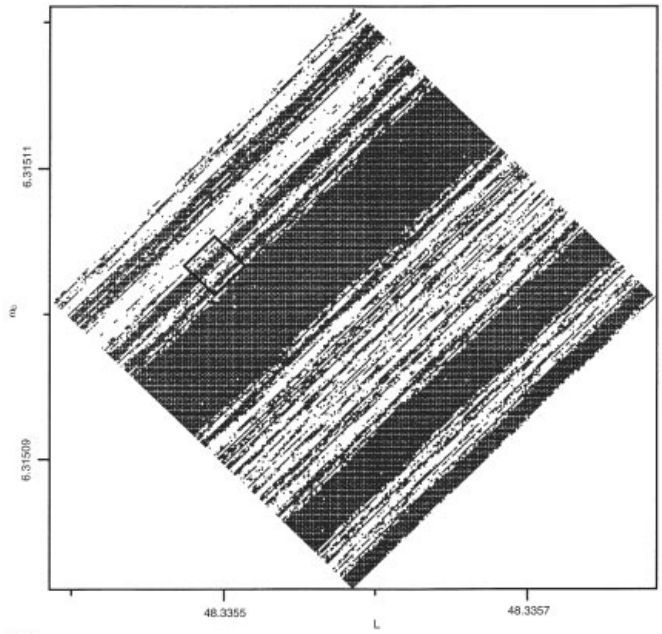

(d)

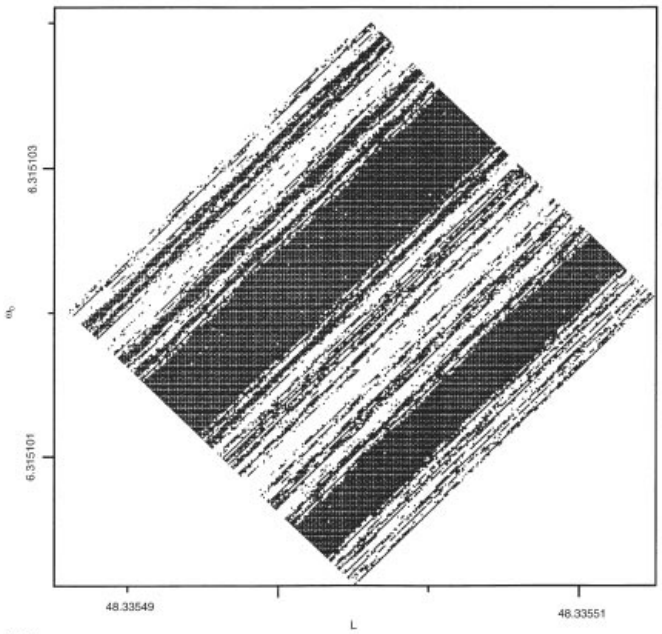

(e)

Fig. 2. Fractal zone boundary between the regular and transiently chaotic zones and its successive magnifications in the phase diagram for the system (1). At each lattice point on the parameter grid the type of solution is shown by a dot (transiently chaotic solution) or blank (regular solution) for the settings time of 20000 cycles. (a) Map of transient chaos for a grid of (L, ω_0) parameters ranging from $L = 45$ to $L = 49$ and from $\omega_0 = 6.222$ to $\omega_0 = 6.48$. (b) Magnification of the boxed region shown in the map (a); (c) Magnification of the boxed region shown in the map (b). (d) Magnification of the boxed region shown in the map (c). (e) Further magnifications as well show a similar pattern.

https://doi.org/10.1017/S0263574799001952 Published online by Cambridge University Press

A segment of this map within the box determined by $48.300 \le L \le 48.400$ and $6.310 \le \omega_0 \le 6.317$ is magnified in Figure 2(b), employing a 400×200 parameter grid.

A segment within the boxed region is magnified in the next map shown in Figure 2(c), with a 250×250 parameter grid, associated with the increments $\Delta L = 1.4 \cdot 10^{-5}$ and $\Delta\omega_0 = 1.4525 \cdot 10^{-6}$. A smaller boxed region in this figure is further magnified in Figure 2(d) with a 250×250 parameter grid, associated with the increments $\Delta L = 7 \cdot 10^{-7}$ and $\Delta\omega_0 = 7.2625 \cdot 10^{-8}$. A smaller boxed region in this figure is further magnified in Figure 2(e), with a 288×288 parameter grid, associated with the increments $\Delta L = 6 \cdot 10^{-8}$ and $\Delta\omega_0 = 6.225 \cdot 10^{-9}$.

Comparison of Figures 2(c), (d) and (e) reveals a repetition of the same pattern at smaller and smaller scales. This clearly indicates that we are seeing a self-similar fractal web that repeats itself indefinitely under higher and higher magnification.

We note that although the Poincare map associated with chaotic transients is not fractal (it consists of a stochastic cloud of unorganized points over a two-dimensional region in parameter space), the boundary between the regular and transiently chaotic zones in the parameter space exhibits the fractal structure. This may be significance because of possibility that some particular narrow tongues intrude deeper into the regular regions.

On the other hand, it is interesting to compare the present phase space map of chaotic transients for the system (1) in the presence of light damping to the previous calculations of basin boundary and transient time initial condition maps associated with Duffing oscillator in the presence of sizeable damping.[23] In the latter case, upon magnification, the fractal structure of the maps appear striated, or a series of narrow parallel lines.

A typical power spectrum of chaotic transients is shown in Figures 3(a), (b). The broad band noise, characteristic of chaotic motion, is the main component of the Fourier spectrum, even though a peak corresponding to the driving frequency ω_0 is still present, but with a rather low amplitude above the noisy background. Furthermore, it is seen that the transiently chaotic Fourier spectrum is characterized by a mean white noise spectrum which approaches a constant value in the limit of low frequencies. Therefore, in analogy to some previous investigations of other systems,[20,27,28] it may be concluded that the appearance of chaotic transients is associated with the loss of phase locking, i.e. that the

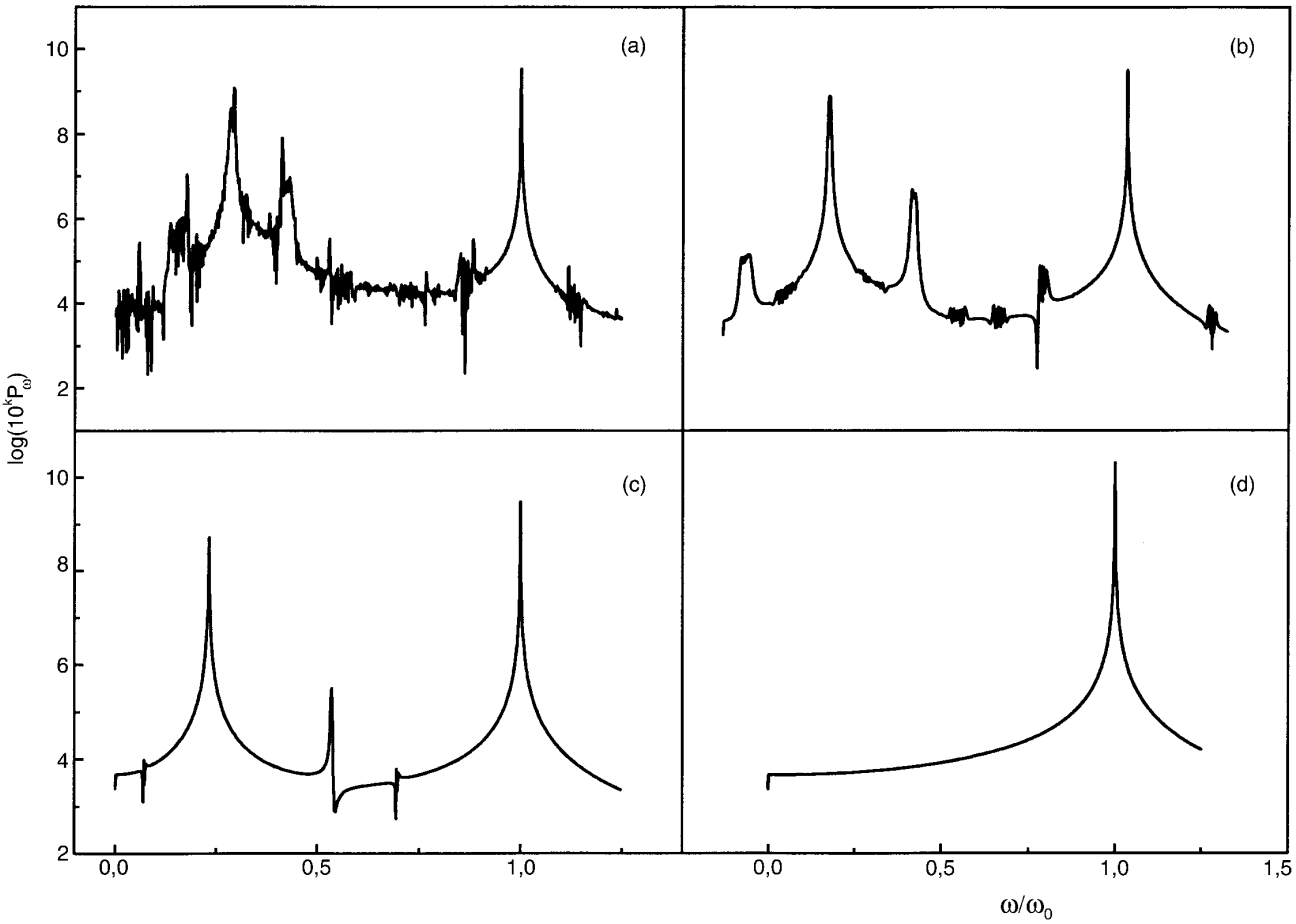

Fig. 3. Time evolution of the power spectrum for $L = 47.98$ at the onset of transient chaos. Power spectra were calculated in the following time intervals: (a) $t = 0$–546.13; (b) $t = 1000$–1546.13; (c) $t = 5000$–5546.13; and (d) $t = 30000$–30546.13.

https://doi.org/10.1017/S0263574799001952 Published online by Cambridge University Press

observed chaotic feature appears to be related to random transitions between different phase-locked states that have become unstable.

During the lifetime of chaotic transient, the power spectrum exhibits the broad band noise (Figures 3(a), (b)), and afterwards the solution settles into a regular pattern, with the power spectrum consisting of one or several pronounced peaks (Figures 3(c), (d)). In the example shown in Figure 3, the chaotic transient asymptotes to the period-1 solution.

After the chaotic transients have died out, the solution asymptotes into one of regular type (quasiperiodic or frequency locked). In Figure 4 the power spectra of such asymptotes are shown for some values of L within the region of onset of transient chaos.

In order to get deeper insight into qualitative behavior of the system associated with the complex transiently chaotic pattern for weak damping, the stable (attractors) and unstable (saddles) periodic orbits were investigated for $L = 48$, $\omega = 2\pi$. The attractors calculated for the $-20 \le x \le 1$, $-2 \le v \le 20$ section of the phase plane are shown in Figure 5(a).

In calculating the saddle points the last two terms on r.h.s. of Eq. (1) had to be neglected. We have found a large number of unstable periodic orbits (saddles). The most pronounced saddle point is the fixed point $x_f = -60.4$, $v_f = 0.9$, with its stable and unstable manifolds (Figure 5(b)). These manifolds intersect each other (Figure 5(b)), producing homoclinic points (homoclinic orbit) which is a necessary and sufficient condition for the appearance of transient chaos.

3. REGION OF CHAOTIC TRANSIENT AND THE CRISIS POINT

The chaotic transient, which for $\omega_0 = 2\pi$ appears first at the value of control parameter $L \approx 48$, persists in a very broad interval up to high values of control parameter L, interrupted

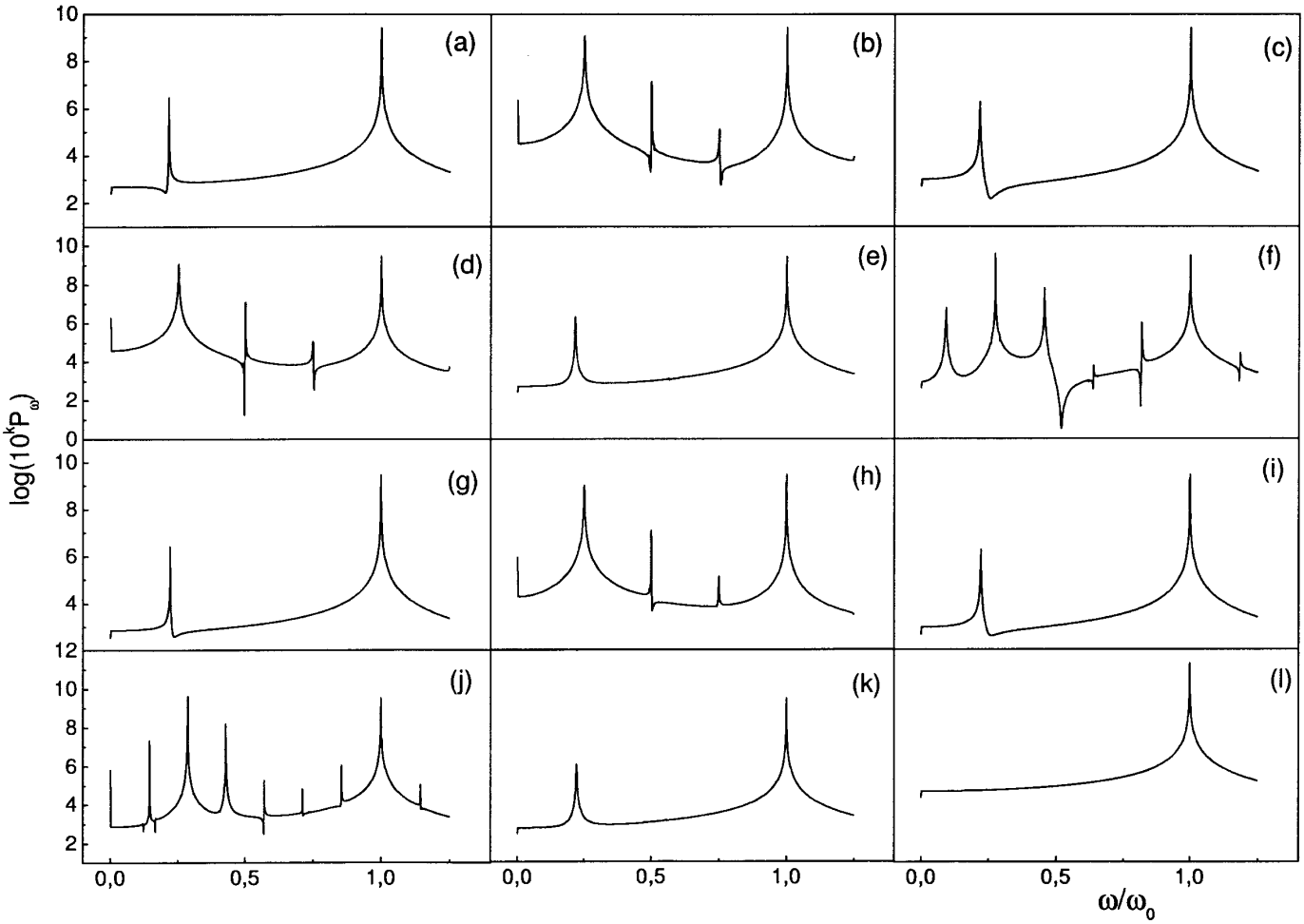

Fig. 4. Power spectra for some values of control parameter near the region of the onset of transient chaos after the chaotic transients have died out, in the time interval $t = 20000$–20546.13. (a) $L = 45.1$ (quasiperiodic); (b) $L = 45.2$ (period-4); (c) $L = 45.3$ (quasiperiodic; (d) $L = 45.8$ (period-4); (e) $L = 45.9$ (quasiperiodic); (f) $L = 46.4$ (period-11); (g) $L = 46.9$ (quasiperiodic); (h) $L = 47.0$ (period-4); (i) $L = 47.4$ (quasiperoidic); (j) $L = 47.5$ (period-7); (k) $L = 48.2$ (quasiperiodic); and (l) $L = 48.3$ (period-13).

https://doi.org/10.1017/S0263574799001952 Published online by Cambridge University Press

by some narrow intervals of periodic windows. A particularly pronounced periodic window is of period 3 in the $L \approx 70$–80 interval of control parameter, as seen from the bifurcation diagram in Figure 6.

In Figure 7 the power spectra are shown for some characteristic values of the control parameter L within the broad region of transient chaos for $\omega_0 = 2\pi$. Power spectra are calculated for each L in the initial time interval from $t = 100$ to $t = 646.13$ and in the time interval from $t = 30000$ to $t = 30546.13$ after the chaotic transients have died out.

At the critical value of control parameter, $L = L_c \approx 4 \cdot 10^4$, the transient chaos turns into sustained chaos. At this point of an inverse crisis, a chaotic transient is converted into chaotic attractor.[19] We see that this crisis point L_c lies far out of the range of values of any significance for engineering purposes.

We note that some dynamical aspects of the Coulomb friction have been previously investigated in mechanical models showing stick-slip motion and chaos.[23–25] In these cases damping was sizeable and accordingly rapid onset of sustained chaos, contrary to the behavior of the present system characterized by weak damping.

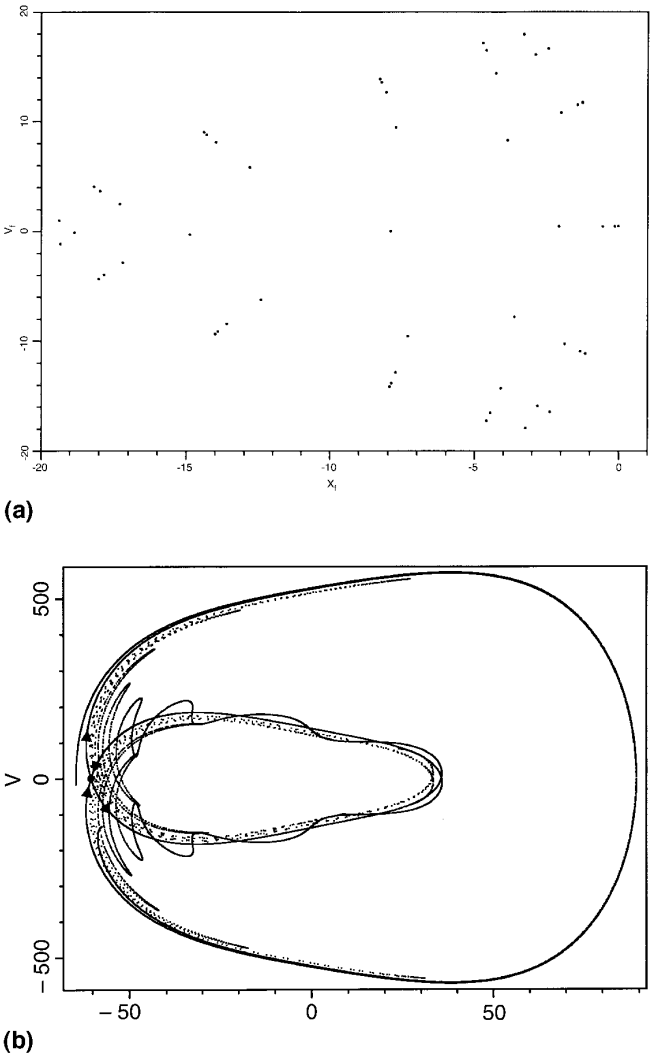

Fig. 5. Stable fixed points (attractors) (a) and unstable fixed point (saddle) with its stable and unstable manifolds (b) for $L = 48$, $\omega = 2\pi$.

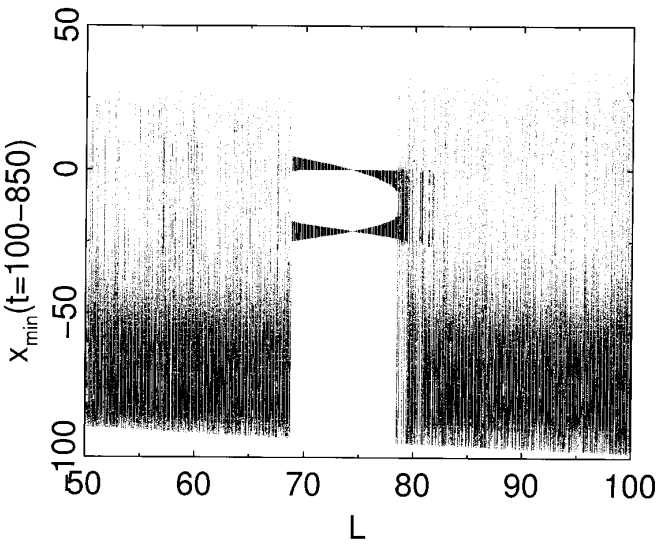

Fig. 6. Bifurcation diagram of (1) in the L-scan of parameterization (I). The calculated values of x_{min} of each oscillation in the time interval from $t = 100$ to $t = 850$ is presented versus L in the range from $L = 50$ to $L = 100$, with increment $\Delta L = 0.08$.

4. CONCLUSIONS

In this work numerical solutions of the system (1), which corresponds to a model of robot with one degree of freedom, have been investigated in the parameter region of transient chaos.

Numerical calculations show that nonlinear phenomena are much richer for this system, characterized by weak damping, than for standard nonlinear system (damped driven pendulum, Duffing oscillator etc.).

We have determined fractal boundaries between the zones of transient chaos and quasiperiodicity, although the Poincaré map of transient chaos is not fractal. It is shown that the range of transient chaos is very broad and the crisis point at which the transient chaos turns into the strange attractor is far removed from the range of significance for engineering purposes. Concluding, the calculations for the present model of a robot with one degree of freedom and reduced to a particular parameter scan indicate that outside of the parameter range of immediate engineering significance the nonlinear effects may be expected to appear in the following order of appearance: two-frequency quasiperiodicity with a period-1 asymptote, Arnold tongues of frequency locking, fractal-type multiple splitting of Arnold tongues, and a very broad region of chaotic transients. Thus, we find that in spite of the rich nonlinear transient phenomena and Arnold tongues, the dynamical system of our robot model exhibits an extreme robustness against sustained chaos.

https://doi.org/10.1017/S0263574799001952 Published online by Cambridge University Press

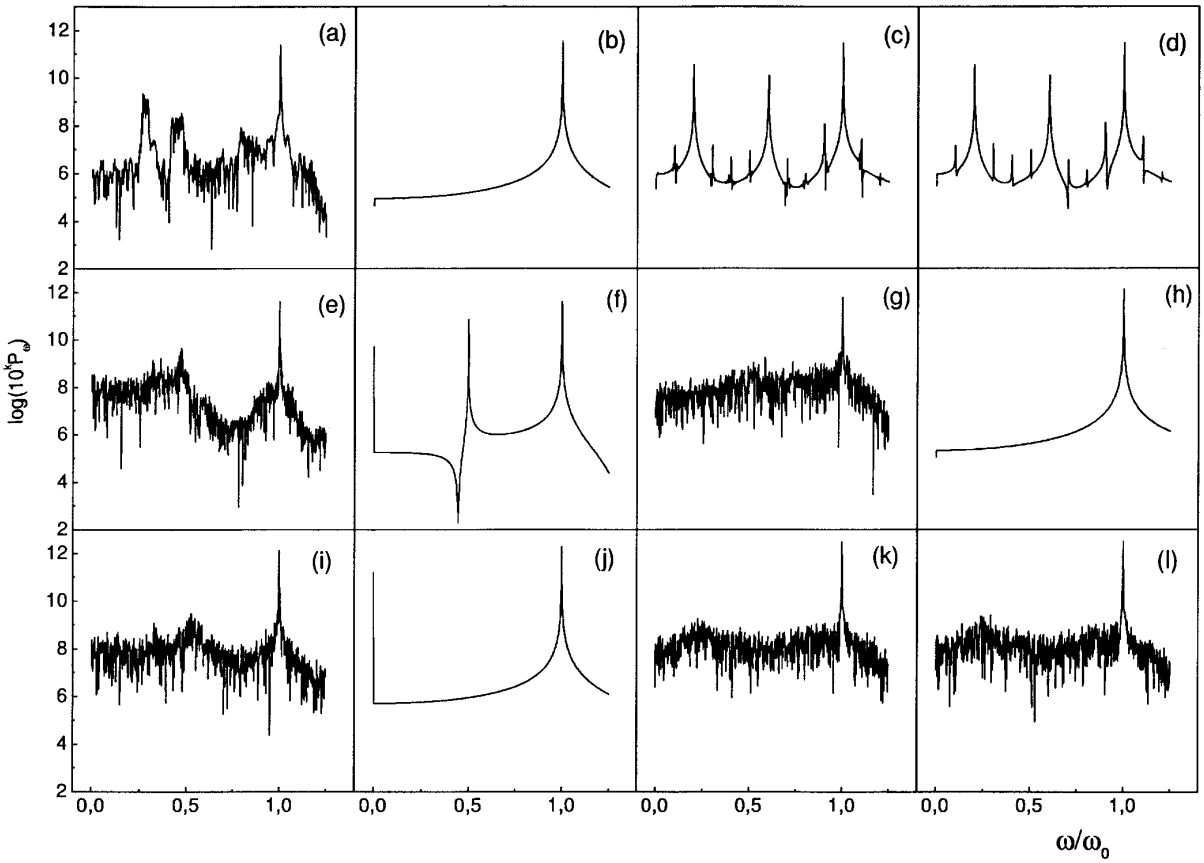

Fig. 7. Power spectra for some values of the control parameter in the range between the point of onset of transient chaos, $L = L_t \approx 48$, and the crisis point ($L = L_c \approx 4.10^4$). Power spectra are calculated for each value of L in the time intervals $t = 100$–646.13 (Figures (a), (c), (e), (g), (i), (k)), and $t = 30000$–30546.13 (Figures (b), (d), (f), (h), (j), (l)) when the chaotic transients have died out. The values of control parameter L are: (a), (b) log $L = 2.8$ (period 1); (c), (d) log $L = 3.2$ (period-10); (e), (f) log $L = 3.4$ (period-2); (g), (h) log $L = 3.8$ (period-1, symmetric); (i), (j) log $L = 4.2$ (period-1, nonsymmetric); and (k), (l) log $L = 4.6$ (strange attractor).

References

1. V. Paar, N. Pavin, N. Paar and B. Novaković, "Nonlinear regular dynamics of a single-degree robot model", *Robotica* **14**, Part 4, 423–431 (1996).
2. J.M.T. Thompson and H.B. Stewart, *Nonlinear Dynamics and Chaos* (Wiley, Chichester, 1988).
3. C. Hayashi, *Nonlinear Oscillations in Physical Systems*. (Princeton University Press, Princeton, N.J., 1985).
4. F.C. Moon, *Chaotic Vibrations* (John Wiley, New York, 1987).
5. W. Szemplinska-Stupnicka, "Chaotic and regular motion in nonlinear vibrating systems", **In:** (W. Szemplinska-Stupnicka, G. Iooss and F.C. Moon, Eds.) *Chaotic Motions in Nonlinear Dynamical Systems* (Springer, Wien, 1988) pp. 51–136.
6. J. Guckenheimer and P. Holmes, *Nonlinear Oscillations, Dynamical Ssytems, and Bifurcation of Vector Fields* (Springer, New York, 1990).
7. A.H. Nayfeh and D.T. Mook, *Nonlinear Oscillations* (Wiley, New York, 1979).
8. P.J. Holmes and F.C. Moon, "Strange attractors and chaos in nonlinear mechanics" *J. Appl. Mech.* **50**, 1021–1032 (1983).
9. U. Parlitz and W. Lauterborn, "Superstructure in the bifurcation set of the Duffing equation $\ddot{x} + d\dot{x} + x + x^3 = f\cos\omega t$", *Phys. Lett.* **A107**, 351–355 (1985).
10. C. Pezeshki and E.H. Dowell, "On chaos and fractal behavior in a generalized Duffing's system" *Physica* **D32**, 194–209 (1988).
11. W. Vance and J. Ross, "A detailed study of forced chemical oscillator: Arnold tongues and bifurcation sets" *J. Chem. Phys.* **91**, 7654–7670 (1989).
12. L. Glass and J. Sun, "Periodic forcing of a limit-cycle oscillator: Fixed points, Arnold tongues, and the global organization of bifurcations" *Phys Rev.* **E50**, 5077–5084 (1994).
13. B. Heimann, H. Loose and G. Schuster, "Contribution to optimal control of an industrial robot" *Proc. 4th CISM-IFTOMM Symp. on Theory and Pract. of Robots and Manipulators* Warsaw (1981) pp. 211–219.
14. R. Paul, *Robot Manipulators: Mathematics, Programming and Control* (MIT Press, Cambridge, Mass., 1981).
15. B. Novaković, "A time and energy optimal control of industrial robots" **In**: (P. Kopacek, I. Troch and K. Desoyer, Eds.) *Theory of Robots, IFAC Proc. Ser.* (Pergamon Press, New York, 1988) pp. 205–210.
16. B. Novaković, "An algorithm for the nonlinear robot control synthesis," *Proc. Int. AMSE Conf.: Signals and Systems* (Brighton, 1989) **Vol. 2**, pp. 12–14.
17. B. Novaković, *Control Methods of Technical Systems* (Školska Knjiga, Zagreb, 1990); F. Csaki, *State Space Methods for Control Systems* (Akademiai Kiado, Budapest, 1977).
18. A. Isidori and A. Ruberti, "On the synthesis of linear input-output responses for non-linear systems" *Syst. Control. Lett.* **4**, 17–22 (1984).
19. C. Grebogi, S.W. McDonald, E. Ott, and J.A. Yorke, "Final state sensitivity: an obstruction to predictability" *Phys. Lett.* **A99**, 415–418 (1983).
20. H. Kantz and P. Grassberger, "Repellers, semiattractors, and long lived chaotic transients," *Physica* **17D**, 75–86 (1985).
21. K.Y. Tsang and M.A. Lieberman, "Transient chaotic distributions in dissipative systems," *Physica* **21D**, 401–414 (1986).
22. F.M. Izrailev, B. Timmermann, and W. Timmermann, "Tran-

https://doi.org/10.1017/S0263574799001952 Published online by Cambridge University Press

sient chaos in a generalized Henon map on the torus," *Phys. Lett.* **A126**, 405–410 (1988).
23. C. Pezeshki and E.H. Dowell, "On chaos and fractal behavior in a generalized Duffing's system," *Physica* **D32**, 194–209 (1988).
24. V. Paar and N. Pavin, "Bursts in Average Lifetime of Transients for Chaotic Logistic Map with a Hole," *Phys Rev.* **E55**, 4112–4115 (1998).
25. V. Paar and N. Pavin, "Intermingled fractal Arnold tongues," *Phys. Rev.* **E57**, 1544–1549 (1998).
26. P. S. Linsay and A.W. Cumming, "Three-frequency quasiperiodicity, phase locking, and the onset of chaos," *Physica* **D40**, 196–217 (1989).
27. D. D'Humieres, M.R. Beasly, B.A. Huberman and A. Libchaber, "Chaotic states and routes to chaos in the forced pendulum," *Phys. Rev.* **A26**, 3483–3496 (1982).
28. M.H. Jensen, P. Bak and T. Bohr, "Transition to chaos by interaction of resonances in dissipative systems. I. Circle maps" *Phys. Rev.* **A30**, 1960–1969 (1984).
29. S. Narayanan and K. Jayaraman, "Chaotic motion in nonlinear system with Coulomb damping," **In:** (W. Schielen, Ed.) *Nonlinear Dynamics in Engineering Systems* (Springer, Berlin, 1990) pp. 217–224.
30. K. Popp and P. Stelter, "Nonlinear oscillations of structures induced by dry friction," **In:** (W. Schielen Ed.) *Nonlinear Dynamics in Engineering Systems* (Springer, Berlin, 1990) pp. 233–240; K. Popp, "Chaotische Bewugungen beim Reibschwinger mit simultaner Selbst - und Fremderregung" *ZAMM-Z. angew. Math. Mech.* **71**, T71–73 (1991).
31. P. Stelter and W. Sextro, "Bifurcations in Dynamic Ssytems with Dry Friction" *Int. Ser. Numerical Math.* **47**, 343–347 (1991).

https://doi.org/10.1017/S0263574799001952 Published online by Cambridge University Press